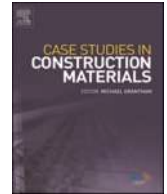
Contents lists available at [ScienceDirect](https://www.sciencedirect.com)

# Case Studies in Construction Materials

journal homepage: [www.elsevier.com/locate/cscm](http://www.elsevier.com/locate/cscm)

## Effect of waste glass bottles-derived nanopowder as slag replacement on mortars with alkali activation: Durability characteristics

Hussein K. Hamzah<sup>a</sup>, Ghasan Fahim Huseien<sup>b,\*</sup>, Mohammad Ali Asaad<sup>c</sup>,  
Dan Paul Georgescu<sup>a</sup>, S.K. Ghoshal<sup>d,\*</sup>, Fahed Alrshoudi<sup>e,\*</sup>

<sup>a</sup> Technical University of Civil Engineering, Bulevardul Lacul Tei 124, sect.2, Bucharest 020396, Romania

<sup>b</sup> Department of Building, School of Design and Environment, National University of Singapore, Singapore 117566, Singapore

<sup>c</sup> Department of Civil Engineering, Iraq University College (IUC), Basra, Iraq

<sup>d</sup> Department of Physics and Laser Centre, AOMRG, Faculty of Science, Universiti Teknologi Malaysia, Skudai 81310, Johor Bahru, Malaysia

<sup>e</sup> Department of Civil Engineering, College of Engineering, King Saud University, Riyadh 11421, Saudi Arabia

### ARTICLE INFO

#### Keywords:

Alkali-activated mortars  
Bottle glass wastes  
Nanoparticles  
Slag  
Drying shrinkage  
Sulphuric acid resistance

### ABSTRACT

Various alkali-activated binders (AABs) incorporated with different industrial wastes emerged as useful environmental affable materials in the construction sectors as alternative to the traditional cement due to their lower CO<sub>2</sub> emission and landfill problems mitigation. The sustainability of concretes is the major global concern in the construction sectors. In this view, the effects of waste glass bottles-derived nanopowder (WGBNP) on the durability characteristics of five batches of alkali-activated mortars (AAMs) with the inclusion of fly ash (FA) and ground blast furnace slag (GBFS) were evaluated. These AAMs were designed via the replacement of GBFS at various WGBNP contents (0%, 5%, 10%, 15% and 20%). Analytical tests were performed to determine the mortars compressive strength, porosity, drying shrinkage, and resistance to aggressive environments. Microstructures characteristics were assessed using XRD measurements. Replacement of GBFS by WGBNP was found to remarkably improve the durability traits of the produced AAMs, solving the environmental and landfill problems. The results indicated that the inclusion of 5% of WGBNP in alkali-activated matrix led to the reduction of porosity and enhancement of the strength and durability performance. Additionally, the replacement of GBFS by WGBNP was found to improve the durability performance in terms of reduced drying shrinkage and increased resistance to sulphuric acid, wearing, and freeze-thaw cycles. The obtained AAMs were demonstrated to be environmentally beneficial regarding the lowering of global warming.

### 1. Introduction

The demand of novel construction materials is ever-increasing for environmental sustainable development that can lessen the carbon footprints significantly. The recent increase in the quantities of industrial and agriculture wastes, primarily called for effective management of solid waste worldwide is a major environmental concern. Due to insufficient space for land-filling and increasing cost for land disposal, it has become essential to recycle and reutilise these industrial wastes [1]. Vast quantities of various kinds of

\* Corresponding authors.

E-mail addresses: [bdggfh@nus.edu.sg](mailto:bdggfh@nus.edu.sg) (G.F. Huseien), [sibkrishna@utm.my](mailto:sibkrishna@utm.my) (S.K. Ghoshal), [alrshoudi@ksu.edu.sa](mailto:alrshoudi@ksu.edu.sa) (F. Alrshoudi).

<https://doi.org/10.1016/j.cscm.2021.e00775>

Received 27 September 2021; Received in revised form 28 October 2021; Accepted 10 November 2021

Available online 12 November 2021

2214-5095/© 2021 The Author(s). Published by Elsevier Ltd. This is an open access article under the CC BY-NC-ND license

(<http://creativecommons.org/licenses/by-nc-nd/4.0/>).

industrial by-products waste materials such as fly ash (FA) [2,3], palm oil fuel ash (POFA) [4], waste ceramic (WC) [5–7], waste glass (WG) [8–11] and ground blast furnace slag (GBFS) [12,13], etc are dumped annually for land-filling. Applications of these waste materials into concrete industry can reduce the disposal concern, making it economical and easily available. Natural resources are declining due to its enormous consumption in the construction industry and manufacturing of cement. Therefore, it has become crucial to seek some options for replacing the traditional cement with alternatives, which could be used as binder in preparing of cement-free concrete [13]. In the past, diverse industrial wastes and by-products like FA, WC, coal bottom ash (CBA), stone dust (SD), GBFS and WG were used as alternative binder to produce the cement-free concretes [14].

As a waste material, GBFS can easily be obtained from the iron industries. It has both cementitious and pozzolanic traits because of high content of calcium oxide (CaO) plus silica and silicon dioxide (SiO<sub>2</sub>). Furthermore, this waste has extensively been exploited in the building industries for improving the strength permanence of the traditional OPC-based concretes [15], alkali-activated [12,16] and geopolymers [17]. Nath et al. [17] assessed the influence of GBFS replacement by varying the contents of FA (0%, 10%, 20% and 30%) on the fresh characteristics of various FA-based geopolymers. The flow of mortar was found to reduce for more than 50% with increased GBFS content as FA replacement from 0% to 30%. With the increase of GBFS content from 0% to 30% both final and early setting times were further reduced. Islam et al. [18] showed that the maximum strength was nearly 66 MPa for 70% of GBFS and 30% of POFA. Nevertheless, high quantities of GBFS addition into the geopolymer mixes could reduce the workability and setting times. The impact of various contents of GBFS/FA on the flowability and mechanical properties of the proposed mortars was evaluated [19]. It was found the replacing FA by 50% of GBFS can achieve the optimum slump. However, the compressive strength (CS) revealed a decreasing tendency with the decrease of GBFS content in the mortar mixtures. Sahana [20] demonstrated that the addition of various levels of GBFS (less than 40%) can elongate the setting times of the mortars, which may further decrease beyond this value, leading to the workability loss of the concrete. Deb et al. [21] interpreted the lowering of this workability at high GBFS level which was ascribed to the strong chemical reaction of GBFS with calcium oxide. Despite the elevated strength performance of these alkali-activated slags the fast setting times and low workability plus large drying shrinkage (DS) limit their wide applications unless reversed [22].

Al-majidi et al. [23] determined the impact of increasing GBFS content on the FA-based geopolymer wherein the workability was found to decrease and setting times (initial and final) as well as hardening was accelerated. At ambient curing condition (23 °C), FA-based geopolymers blended with GBFS or OPC was discerned to reduce the setting time to a value comparable to that of OPC. The workability was measured in terms of the flow of mortars, which showed slight decrease due to the presence of the additives and faster rate of setting [24]. Al-Majidi et al. [23] cured the FA-based geopolymers at ambient temperature to determine the strength performance. With the increasing ratios of GBFS to binder in the geopolymer mixes, the strength performance was appreciably improved. Increase of GBFS level from 10% to 50% was found to enhance the 28 days' compressive strength (CS) from 18.45 to 48 MPa. In addition, the impact of GBFS inclusion in the geopolymers to improve the flexural strength (FS) and tensile strength (TS) cured at ambient temperature was comparable to the strength development. GBFS content of 40% showed optimum mechanical performance with 6 MPa (for FS) and 3 MPa (for TS). Nath et al. [24] studied the impact of GBFS or OPC inclusion on the CS of FA-based geopolymer. The CS of the geopolymer was increased with the increase of the binder content for FA blended with 10% GBFS or OPC.

Increasing level of GBFS in FA-based geopolymer mixture was found to improve the microstructure and enhanced the structural density and lowered the porosity [23]. Li and liu [25] reported that by blending the slag with FA-based geopolymer can enhance the durability properties of mortar/concrete and showed good resistance to permeation. GBFS was blended with FA-based geopolymer to elevate the resistance against elevated temperatures [26] and sodium sulphate attack [27]. Moreover, it suffered deterioration in magnesium sulphate attack [27] and the DS became higher [28]. Several studies showed that the geopolymers incorporated with GBFS have lower durability performance at elevated temperatures [29], against acid attacks [30], reduced porosity and DS [19]. Regarding to resistance to acid attack, the weight loss of the investigated specimens was found to decrease from 2.2 to less than 0.25% due to the reduction of corresponding GBFS content from 50% to 10%. Additionally, the worsening rate was observed to reduce with the increase of slag contents in the proposed blends. The microstructures analyses of the FA-based geopolymers containing slag showed typically the formation of glassy hydration products containing CaO. The produced gel became more compact with the increase of slag level in the mortars, thus enhancing the durability [17].

Nowadays, the climate change is highly influenced by the amount of by-product and agricultural wastes [31–33]. As reported by American Environmental Protection Agency (AEPA), the total quantity of waste materials in 2015 augmented to 262 MT from 8 MT in 1960. In 2015, it was reported that the recycled waste materials limited to 26% and 9% was composted. Furthermore, 13% was burnt to recover the energy and 52% was used as landfills disposal. Batteries and steel were the most recyclable wastes. Annually, several types of glass wastes are disposed to the landfill and only 34% are recycled. The chemical composition and physical properties of glass play the main role on its recycling [34,35]. Usually, the glass accessories are composed of sand (as primary component for silica), soda ash (SA), limestones and cullet. SA is often added in some recycling products to lower the melting point. The melting points and colours of the glasses depend on their chemical composition and thus the recycling of the glass bottles are difficult if they are not classified according to their colours [36,37]. The other reason behind the inefficient recycling of the glass is related to their unknown sources where people randomly mix the glass bottles and containers during the gathering (without proper sorting based on their colours and categories). The process of sorting these mixed glass containers are very inefficient and labour intensive. In addition, the presence of impurities or contaminants disallows their effectual recycling. In fact, prior to the recycling, these glass containers, or accessories must be devoid from any chemical residues, medicine particles or other toxic materials.

Glasses are a hard and brittle substance, usually transparent or translucent. Depending on their main composition many types of glasses exist including soda-lime, vitreous-silica, alkali-silicate, borosilicate, borate, tellurite, phosphate, germanate, tungstate, lead, barium, and aluminosilicate. Different types of glasses (called amorphous system) are produced via the melt-quenching method by mixing CaCO<sub>3</sub>, SiO<sub>2</sub>, Na<sub>2</sub>CO<sub>3</sub>, and CaMg(CO<sub>3</sub>)<sub>2</sub> in the high temperature furnace (1500–2000 °C) [38]. Small amounts of additives are

often added during the production of glasses to give glasses different colours or to improve specific properties [39]. It was reported [40], that the recycling of this waste by converting it to aggregate not only saves landfill space but also reduces the demand for extraction of natural raw material for construction activity. Park et al. [41] reported that the CS, TS, and FS of concrete made from WG as fine aggregates replacement reveals declining trend with increase of WG contents. According to Topcu and Canbaz [42], concrete made from WG as coarse aggregates replacement in the matrix displays declining trend in the value of CS, TS, and FS with increasing of WG contents.

Numerous studies [8,43–45] have been carried out to successfully recycle the waste glasses as the cullet in the glass production, raw materials for abrasives manufacturing, sands blasting, and aggregates supernumerary in the concretes, in the pavement, roads and parking lot construction, production of glass pellets/beads utilised in lighting the reflective paint for the highways, fibre-glass fabrication, and fractionators for matches and ammunition firing [46]. Zainab and Enas [47] showed that recycled WG (at various contents of 10%, 15% and 20%) can partially be used in the concretes as effective substitute to the fine aggregates. The results proved that at 28 days, the pozzolanic strength achieved 80% and the optimum percentage of waste glass is 20% that gives the maximum value of compressive and flexural strength. Four kinds of glasses with varying particles size was used as cement replacement (at 20%) to design some concretes, wherein it was shown that tinier particles were more reactive to  $\text{Ca}(\text{OH})_2$  present in the cement [48]. Concrete cured for 7 days revealed lower CS than the one cured for 28 days. It was reported that [49] it is feasible to use fine ground glass from waste as OPC partial replacement in concrete production. For this purpose, lime glasses were powdered and tested to examine their pozzolanic efficiency where 30% of OPC was replaced by such glass powder. The results revealed the highest CS for 30% replacement compared to other level of replacement and control sample. It was indicated that mortar specimens prepared using glass powder having particle size less than  $38\ \mu\text{m}$  achieved the pozzolanic requirements [50].

Over the years, waste glass bottles (WGB) and glass windows have widely been used to make modified concretes. It has been realised that the use of fine glass powders as the complementary cementitious component is more economic and environmental friendly. Meanwhile, glass-cullet has also been used in the concrete as a substitute agent for the fine aggregates [51]. Based on a review conducted by Shi and Zheng [48], it was observed reduction in the usages of energy, resource materials, wears and tears on the machineries with the implementation of the recycled aggregates in the glass manufacturing. Yet, it is not possible to recycle all types of glasses to make new glasses due to the presence of contaminants, price and colour mixing. It is essential to produce new types of glasses by mixing various waste glasses for developing new marketing and applications. In this regard, the uses of such glass wastes in the construction industries can be a profitable option due to the substantial demand of massive amounts with moderate qualities. The major applications of the waste glasses in the civil engineering field are the partial substitution of natural aggregates in the asphalt concretes, pipes bedding, and gas-venting system in the landfills and gravels backfill for the drainage system. Jani and Hogland [44] overviewed in detail the manufacturing of WG-based cements and concretes. The disposal of solid waste including waste glass was claimed to cause serious environmental pollutions. It was argued that to surmount the negative environmental effects of the waste glasses the best strategy is to recycle them which enables conserving the natural resources, minimising the landfills, saving the energy and cost.

In the development of sustainable concretes, nanosilica with unique morphologies is an exceptional nanomaterial used widely in the ultra-high performance concretes (UHPCs). Generally, nanosilica is produced from micron size silica particles. The strong chemical activity shown by nanosilica in the UHPCs is analogous to the silica-fume or micro-silica particles due to their strengths and durability performance enhancement [52–54]. Qing and Zenan [53] showed that concretes with nanosilica can achieve early strength better compared to silica-fume. The inclusion of nanosilica into the concretes can improve the workability at the minimum level of super-plasticizer. Furthermore, the size of nanosilica particles can serve as super-filler in the concretes, producing dense and refined micro-voids and achieving elegant microstructures [55]. On top, nanosilica has excellent ability to regulate water to cement proportion with tailored strength properties. It was shown that the concrete incorporated with nanosilica at some level [56] can achieve improved strength performance analogous to cement replacement. Approximately 20–30% of the OPC uses can be reduced through nanosilica implementation, indicating the possibility of sustainable development in the building industries. Regarding the applications of self-repairing concretes, nanosilica was shown to strongly react with  $\text{Ca}(\text{OH})_2$ , formulating C-S-H gel [57–60]. Present self-healing concretes use nanosilica as extra mineral component or nanoencapsulated agent to achieve enhanced performance. Nonetheless, wider applications of nanosilica is limited due to its high cost and accessibility in some countries wherein this material is imported for developing the nanotechnology-based concrete industries [61].

Considering the negative impacts of GBFS on the durability properties this study emphasized the replacement of GBFS by WGBNP in an eco-friendly way to create some AAMs useful for the construction sector. The durability properties of the achieved AAMs including the water absorption (WA), carbonation depth (CD), resistance to freezing-thawing cycles, abrasion resistance (AR) and performance against aggressive environments were evaluated as a function of WGBNP contents as replacement of GBFS. In addition, the microstructural analyses of the AAMs were carried out via the XRD measurements to get a better understanding of the mechanism responsible for the performance improvement due to WGBNP inclusion.

## 2. Methodology

### 2.1. Materials

Waste FA (class F enriched with aluminosilicate) was procured from a thermal plant located in Johor (Malaysia) to design the mortar mixes (AABs). It satisfied the ASTM C618 requirements for N class pozzolan and F class fly ash and appears grey in colour. These AABs were produced from clean GBFS procured from a Malaysian company (Ipoh) without addition chemical treatments. This slag

possesses both cementitious and pozzolanic properties. It is considered to be different from other supplementary cementitious materials. The GBFS displayed off-white colour when mixed with water due to the occurrence of hydraulic reactions. GBFS was comprised of nearly 90% of calcium silicate and alumina, thus fulfilling the requisite of the pozzolanic substance as per ASTM C618 specification. In addition, WBG was collected from food industry and from same resource. First, the bottles cleaned then dried before process for crushing stage in the lab. The preparation stages of the nanopowder from WBG are illustrated in Fig. 1.

According to ASTM C33, the washed-dry river sand with the maximum grain size of 2.36 mm was utilised as fine aggregates for the AAMs preparation. The estimated specific gravity (SSG) and fineness modulus (SFM) of the aggregates were 2.6 and 2.9, respectively. Two-parts of alkaline activator solutions (NaOH and Na<sub>2</sub>SiO<sub>3</sub>) were adopted to prepare the proposed mortar mixtures. Sodium hydroxide with concentration of 2 (supplied by the quality reagent chemical, QREC, Asia, Malaysia) was used for all mixtures activation. The sodium silicate solution containing 14.7% of Na<sub>2</sub>O, 29.5% of SiO<sub>2</sub> and 55.8% of H<sub>2</sub>O (QREC, Asia, Malaysia) was mixed with NaOH with the ratio of 0.75 to prepare the final alkaline activator solution. Fig. 2 displays the alkaline activator solution (AAS) preparation procedure.

## 2.2. Mix design

Based on the trial mixes, for all AAMs the optimum ratio of binder to sand was 0.30 and AAS to binder was 0.40. Three types of waste materials were used to prepare the AAMs mix design. Ternary blended contents such as FA, GBFS and WGBNP were taken to determine the influence of nanomaterials on the geopolymerization process and engineering properties of AAMs. The minimum content of GBFS as a source of CaO was kept to a minimum of 10% in replacement process and maximum of 30%. Table 1 shows the constant concentration of sodium hydroxide, sodium silicate to sodium hydroxide, and alkaline activator solution modulus (Ms) of 2, 0.75 and 1.2, respectively. According to ASTM C 109, five batches of AAMs were prepared with various replacement levels of GBFS by WGBNP. First, the prepared ternary binders mixed in dry condition for 2 min then followed by the addition of river sand and mixing for another 3 min to achieve the homogeneous mix. Then, the mixed binder and filler for each mixture was activated with two-part of AAS followed by mixing for 3 min. The fresh mortars were poured in the moulds in two layers and then left for 1 day at 24 ± 1.5 °C with 75% of relative humidity before being de-mould.

## 2.3. Tests

Hardened properties of the AAMs were tested (following the ASTM C579) by mixing, casting and curing. In this process, cubical specimens of size (50 mm × 50 mm × 50 mm) were casted to test the CS, porosity, resistance to abrasion, sulphuric acid and



Fig. 1. Preparation stages of WGBNP.



Fig. 2. Procedure for the alkaline activator solution preparation.

Table 1

Details of various AAMs designed with WBGNP and GBFS.

Mix	Ternary binder, mass%			Binder to sand	AAS to binder	Total water in AAS	Sodium silicate to sodium hydroxide	AAS modulus (Ms)
	FA	GBFS	WBGNP					
AAMs <sub>1</sub>	70	30	0	0.30	0.40	76.8	0.75	1.2
AAMs <sub>2</sub>		25	5					
AAMs <sub>3</sub>		20	10					
AAMs <sub>4</sub>		15	15					
AAMs <sub>5</sub>		10	20					

carbonation depth. Prism-like specimens of size (40 mm × 40 mm × 80 mm) were utilised to measure the resistance against freezing-thawing cycles. The DS test was performed using prism-like specimens of size (25 mm × 25 mm × 225 mm). For each test, the average value of three specimens was considered. The porosity of the proposed mortars was determined using the water absorption (WA) experiment. Following ASTM C 642 specification water absorption test is performed. The specimens were casted in (50 mm × 50 mm × 50 mm) mould. After the specimens were matured, they were immersed in water for a day at 27 °C. Next, the weight of the specimens ( $W_s$  in g) was measured after they hanged and immersed totally inside water. After the saturation, the tested mortars were oven-dried for a day at 105 °C followed by the weighing ( $W_d$  in g). The values of WA percentage of the mortars were calculated using the relation:

$$WA (\%) = [(W_s - W_d)/W_d] \times 100 \quad (1)$$

In accordance to the ASTM C157 standard, the DS test was carried out. Three sets of casted mortars in the form of prism were used to evaluate the effect of WBGNP contents on DS values of AAMs. The ASTM C192 was followed to make the mortars for testing after curing under ambient state for a day (at 23 °C with relative humidity of 50%). To measure the alteration of length in the specimens they were embedded with stainless steel studs. After casting for a day, the mortars were de-mould and then kept at ambient condition. The readings are taken by using demec metre at early and late ages. The length change ( $\Delta l_x$  in %) was estimated using the relation:

$$\Delta l_x = \frac{CRD - \text{initial CRD}}{G} \times 100 \quad (2)$$

where CRD is the difference between comparator reading of the specimen and reference bar at any age; G is the fixed gauge length of 100 mm.

Following the recommended procedure (BS 1881-210:2013), the accelerated carbonation depth (CD) measurement of the AAMs was conducted within a compartment (plastic box) where the specimens were exposed to CO<sub>2</sub> (from a cylinder) for 3 min (at 600 mm of mercury pressure with of 55–60%). Next, the specimens were exposed to CO<sub>2</sub> inside the chamber for 28 and 60 days (at 26 °C and 4% pressure). The gas pressure was constantly monitored using a digital gauge placed between the carbon dioxide gas cylinder and plastic container. In this experiment, three cubical mortar specimens with the dimensions of 50 × 50 mm were observed. After 90 days of CO<sub>2</sub> exposure, the concrete cylinders were broken in 2 pieces, and the cross-sections were sprayed with a 0.2% phenolphthalein solution. Phenolphthalein turns non-carbonated concrete pink and remains colourless in carbonated concrete and the carbonation depth was thus determined.

The abrasion resistances of the AAMs were obtained at various curing ages (from 1 to 56 days under the dry state following the IS 1237-1980 wherein 4 points were selected to determine each specimen's thickness. The thickness difference of each mortar specimen was recorded after and before the test to evaluate the degree of abrasion. The measured values were compared with the estimated

average in the thickness decrease using the expression:

$$T = \frac{[(W_1 - W_2) \times V_1]}{(W_1 \times A)} \quad (3)$$

where T denotes the average thickness loss (mm),  $W_1$  and  $W_2$  (g) are the corresponding pre and post-abrasion weight of the mortar,  $V_1$  and A are the volume ( $\text{mm}^3$ ) and surface area ( $\text{mm}^2$ ) of the mortar before the abrasion test.

The durability properties of the mortars with at least 300 freeze-thaw cycles were tested following the ASTM C666. The mortars temperature were varied from 5 to  $-20^\circ\text{C}$  (cooling over 75% of the freeze-thaw cycles time) and in reverse order (heating over 25% of the freeze-thaw cycles time) over 5 h for each cycle to attain the condition. Specimens were evaluated in term virtual appearance of strength and weight loss after each 50 cycles. According to ASTM C 267-01, mortar specimens with 50 mm size cube cured for 28 days are used to measure the resistance of proposed binders to sulphuric acid attack. The mortars were maintained in the atmospheric condition for about 2 days to get the steady weight before being submerged in  $\text{H}_2\text{SO}_4$  solution. At testing time (180 and 365 days), all specimens were taken out and the surfaces were cleaned to eliminate the loosely bound substances, thus removing the surface materials. After the mortars were dried, the CS and weight changes were measured to calculate the corresponding average loss (%). The procedure of resistance to acid attack is shown in Fig. 3.

The mineral compositions and crystallinity of the binders was examined using XRD technique. This test provided the information of the structures, phases, preferred crystal orientations, and structural parameters of the AAMs. In this study, the specimens were collected from AAMs that were subjected to the CS test at 365 days of age, and then ground to make powder. These specimens were scanned over the  $2\theta$  range of  $5-90^\circ$  with a step size of  $0.020^\circ$  and time per scan of 15.4 s.

### 3. Results and discussion

#### 3.1. Chemical, physical and mineral properties of raw materials

The chemical compositions of FA, GBFS and WGBNP were determined using X-ray fluorescence spectroscopy (XRF). Table 2 presents the XRF results of the raw materials used to prepare the AAMs. Silica was found to be the main oxide in the chemical composition of FA (57.2%) and WGBNP (69.2%) compared to GBFS (30.8%). FA and WGBNP contained higher amount of alumina oxide than GBFS. Additionally, calcium oxide was the main chemical composition of GBFS about 51.8% compared to 5.2% and 3.2% found in FA and WGBNP, respectively. However, the loss on ignition (LOI) for FA, WGBNP and GBFS was 0.12%, 0.16% and 0.22%, respectively.

Table 3 displays the physical characteristics of the raw substances including FA (grey in colour), GBFS (off-white in colour), and WGBNP (light-grey in colour) used to design the proposed AABs. The distributions of particles size of the raw constituents such as FA, WGBNP and GBFS were measured by the particle size analyzer wherein the obtained corresponding median particles' sizes were 10,000, 12,800 and 80 nm. In addition, the particles' sizes of about 100% of FA and GBFS were less than  $45\ \mu\text{m}$  and 100% of WGBNP was  $1\ \mu\text{m}$ . These sizes satisfied the pozzolanic requisite of ASTM C618 with 66% passed at  $45\ \mu\text{m}$  [62]. To determine the physical characteristics of the constituents, their BET surface were measured. Table 2 enlists their specific surface area and physical properties. For FA and GBFS raw materials, it was observed that the specific surface area of FA revealed the highest value of  $18.1\ \text{m}^2/\text{g}$  compared to GBFS which was estimated to be  $13.6\ \text{m}^2/\text{g}$ . The fine size and light specific gravity of FA have influenced on the surface area test which showed the highest value. However, the WGBNP presented specific surface area of  $206\ \text{m}^2/\text{g}$  and specific gravity of 1.02.

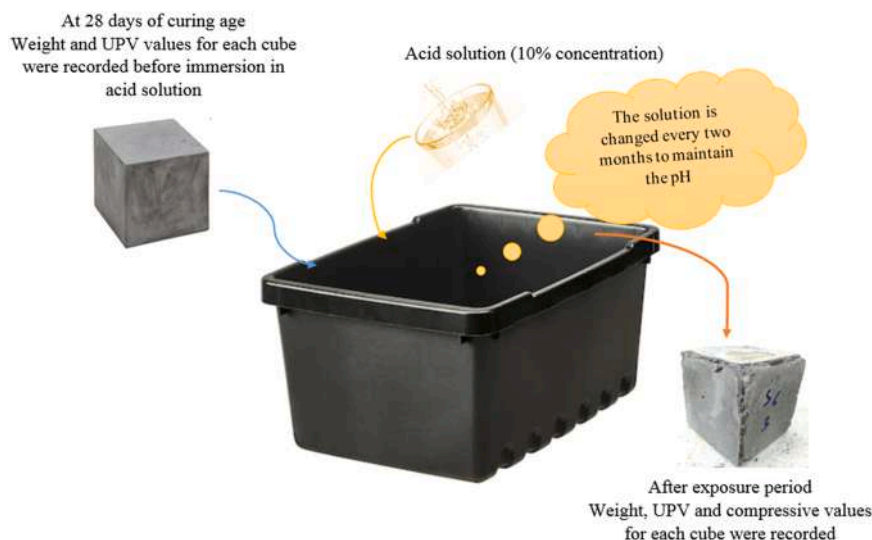


Fig. 3. Mortars' resistance against acid attack test.

**Table 2**

Chemical composition of raw materials based binders (weight %).

Materials	SiO <sub>2</sub>	CaO	Al <sub>2</sub> O <sub>3</sub>	MgO	Fe <sub>2</sub> O <sub>3</sub>	K <sub>2</sub> O	Na <sub>2</sub> O	SO <sub>3</sub>	LOI
WGBNP	69.2	3.2	13.9	0.7	0.2	–	–	4.1	0.16
FA	57.2	5.2	28.8	1.6	3.7	0.9	0.1	0.1	0.22
GBFS	30.8	51.8	10.9	4.6	0.6	0.4	0.5	–	0.16

**Table 3**

Physical properties of FA, GBFS and WGBNP.

Materials	Colour	Particle size (µm)	Specific surface area (m <sup>2</sup> /g)	Specific gravity
FA	Grey	10	18.2	2.20
GBFS	Off-white	12.8	13.6	2.89
WGBNP	Light-grey	0.08	206	1.02

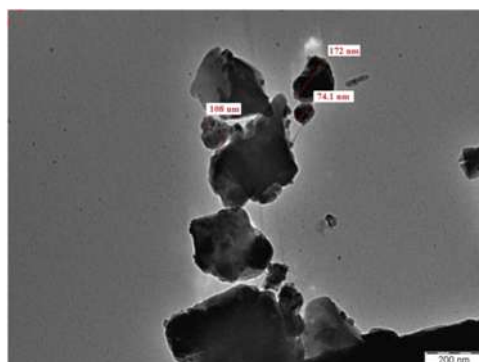
Likewise, the nano particle of glass powder effect on surface area test and presented very high value compared to FA and GBFS.

The particle size of WGBNP was estimated using the transmission electron microscopy (TEM) and high resolution transmission electron microscope (HR-TEM, JEOL JEM-ARM 200F model. At smaller magnifications, the TEM image contrast was due to the absorption of electrons, thickness, and composition of the material. At higher magnifications the complex wave interactions modulated the intensity of the micrographs, requiring expert analysis of the observed images. In the TEM analysis, a concentrated beam of electrons passes through a very thin sample and depending on the electron density various areas of the powder interact with the beam differently, resulting in an image. The produced micrograph represents the gradient areas of the electron density. To record the TEM and HR-TEM micrographs, about 15 g of WGBNP was oven-dried for 3 h at  $110 \pm 5$  °C to remove all the moisture. Until the time of testing, the sample was then kept in vacuum container to avoid the absorption of moisture from the atmosphere. Fig. 4 shows the TEM micrograph of WGBNP with estimated medium size of particles 80 nm which was consistent with the one found in nanosilica-based compounds.

Fig. 5 illustrates the X-ray diffraction (XRD) patterns of the raw materials including WGBNP, FA and GBFS. The XRD profile of WGBNP was largely comprised of amorphous halo with very low intensity quartz peaks between 28.6° and 31.2°. Conversely, FA revealed intense crystalline XRD peaks between 15° and 61° wherein the sharp peaks at 15, 28.4 and 41.1° were due to the existence of alumina/silica crystallites. GBFS due to its glassy nature did not reveal any crystalline Bragg's peak. The existence of reactive Ca/Si-based materials at high concentration is the main benefits of using GBFS, making GBFS potential for the fabrication of AAMs.

### 3.2. Compressive strength

Fig. 6 displays the impact of WGBNP content on the CS development of mortars at 28 days of curing age. The CS showed a monotonic increase with the increase of WGBNP content from 0% to 5%. The CS value was increased from 56 MPa to 65 MPa when the WGBNP content was raised from 0% to 5%. Nonetheless, once the WGBNP content exceeded 5%, the CS was gradually decreased, reaching to 42.1 MPa at 20% of WGBNP content. The high compressive strength of prepared mortars was attributed to GBFS alkali-activated reaction and formation of more C-A-S-H gel, giving rise to minerals known as tobermorites enhanced the AAMs' compressive strength [63,64]. Preparation of the nanosilica incorporated cement and free cement binders based concretes as sustainable building materials can be used to enhance their microstructures and bulk characteristics [65–67]. It has become known that as a result to the high specific surface area-to-volume ratio of nanomaterials, their presence promotes and accelerates the chemical reaction rate of concrete mixture. It seems that the increase in strength was primarily due to the technique used to produce nanosilica and dispersion in WGBNP. The role of various nanomaterials in enhancement the strength indexes of a nanostructures-modified concrete

**Fig. 4.** TEM image of WGBNP.

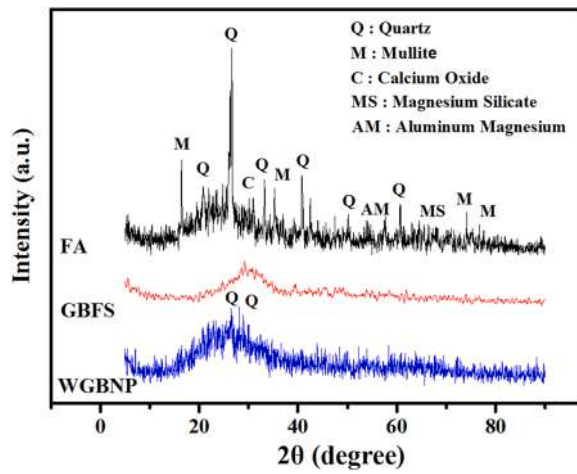


Fig. 5. XRD patterns of FA, GBFS and WGBNP.

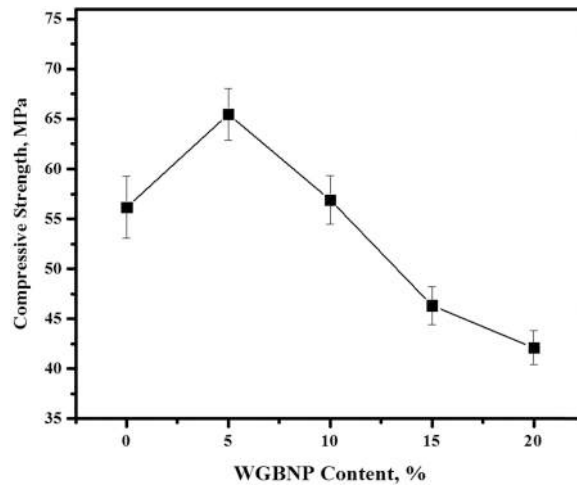


Fig. 6. Effect of WGBNP content on the CS development of mortars at 28 days of curing age.

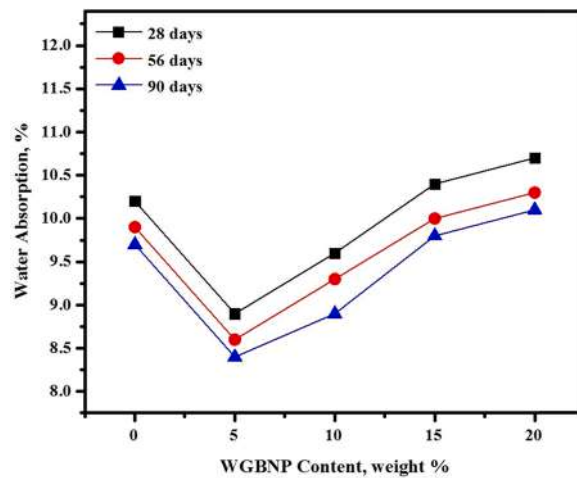


Fig. 7. Influence of WGBNP contents on the WA of mortars at various curing ages.

system was investigated by a group of researchers [68–78]. This increase in the compressive strength was due to the improved filling effect, additional nucleation sites provided by nanoparticles, extra C-A-S-H gel formulation and reducing pores volume, that reflected positively on the compressive strength. The studies showed that the CS of the concrete continued to increase up to 8% of nano SiO<sub>2</sub> addition and dropped thereafter [18,21]. Several researchers [14,16] showed that the addition of 4–6% of nanoSiO<sub>2</sub> by weight in place of FA may reduce the amount of WA capacity, making the structure denser. Consequently, the CS of the concrete was enhanced. However, the reduction of the CS for the specimens prepared with WBGNP content above 10% may be due to high water demand, thus producing an adverse effect on the hydration process.

### 3.3. Water absorption

Fig. 7 shows the influence of WBGNP contents as GBFS replacement on the WA of mortars at various curing ages. The values of WA for all the mortars were found to drop with the increase of curing ages. At each age, the WA of tested specimens was highly influenced by the WBGNP content as GBFS replacement. At age of 28 days, the increasing level of WBGNP in alkali-activated matrix from 0% to 5% led to drop the WA value from 10.2% to 8.9%, respectively. Nonetheless, with the increase of WBGNP contents from 10% to 20% the corresponding WA value was increased from 9.6% to 10.6%. Similar trend of results was obtained for the specimens evaluated at 56 days of curing age. The lowest value of WA (8.6%) was observed for the specimen made using 5% of WBGNP as GBFS replacement. For the specimens evaluated at 90 days of curing age, with the increase of WBGNP content from 0% to 20% the corresponding WA was increased from 9.7% to 10.1%. The inclusion 5% of WBGNP led to enhance the microstructure morphology, reducing the pores density and improving the strength performance, thus lowering the WA compared to control sample and other mixtures. This observation can be explained using two factors. First, with the increase of WBGNP level from 0% to 5% more dense C-A-S-H gel was formulated, thus improving the CS and lowering the WA of the mortar. In addition, the mortars prepared with 5% of WBGNP the porosity was reduced to nearly 12.7% than the control sample. This clearly indicated the significant impact of WBGNP presence on the hydration properties of the mortars. In general, the nucleation mechanism of WBGNP enables the formulation of C-S-H gels, thus improving the hydration reaction in the mortar matrix that allowed to fill large number of pores [79]. Consequently, the AAMs porosity was first reduced with the increase of WBGNP contents (at 5% and 10%). Second, with the increase of air volume in the mortars due to the inclusion of WBGNP, the specimens' porosity was again enhanced as the C-S-H formation was inadequate to balance the pores that trapped air in the fresh mortars. Accordingly, these two opposing mechanism decided the optimum concentration of WBGNP in the mortars, making the porosity level minimum.

Fig. 8 illustrates the correlation between the WA and CS of AAMs prepared with various WBGNP contents as GBFS replacement. A reciprocal relation was exhibited between WA and CS. At 28 days of age, the WA was reduced from 10.7% to 8.9% as the strength of tested specimens increased from 42.1 to 65.5 MPa with the decrease in WBGNP replaced GBFS from 20% to 5%, respectively. Present results are similar to the one obtained by previous researchers [80,81] wherein the WA of the AAMs was shown to decrease with the increase of its CS. The measured data on CS and WA was correlated using the following linear regression relation showed excellent confidence (with R<sup>2</sup> of 0.86):

$$WA = -0.0752 CS + 13.837 \quad (4)$$

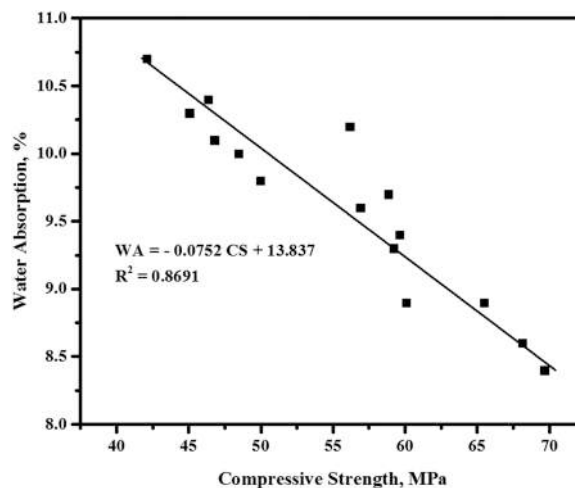


Fig. 8. WA and CS correlation for the obtained AAMs.

### 3.4. Drying shrinkage

Fig. 9 displays the mean DS values of the AAMs incorporated with FA, GBFS and WBGNP. In the early curing age till 28 days, irrespective of the WBGNP contents the DS values of the AAMs were rapidly dropped, indicating an inverse correlation between DS and WBGNP contents. Additionally, the values of DS of the AAMs were very high in-between 3 and 28 days. The DS values were decreased from 269 macrostrain to 244 macrostrain with the corresponding increase of WBGNP level from 0% to 20% in the AAM matrix at 28 days of curing age. Comparable results were obtained after 56 and 90 days. At 56 days, the DS values of the mortars were in the range of 288–254 macrostrain wherein the mortar containing lowest amount of GBFS displayed the lowest DS value. Finally, at 90 days the values of DS of the AAMs made with 0–20% of WBGNP as GBFS replacement was correspondingly decreased from 297 to 266 macrostrain. The observed decrease in the DS values with the increase of WBGNP level was mainly due to the formation of extremely interlinked capillary-like networks within the mortars matrix. Conversely, the replacement of GBFS by different amounts of WBGNP enabled to drop the CaO content in the mortars because of WBGNP has lower Ca (3.16%) level than GBFS (51.8%). This drop in the CaO level in turn lowered the rate of hydration reaction in the AABs. Consequently, the mortars containing high amounts of WBGNP exhibited lesser DS than the mortar prepared with 100% of GBFS (control sample) [82].

### 3.5. Carbonation depth

The CD readings of AAMs containing various levels of WBGNP were recorded after the exposure to CO<sub>2</sub> for 90 days (Fig. 10). Three AAMs specimens were selected to measure the impact of WBGNP content on CD using phenolphthalein. Compared to the control specimens (0% of WBGNP), the mortars made with WBGNP showed an enhancement in the durability. The CD of the mortar prepared with 5% of WBGNP as GBFS replacement was lower (7.6 mm) compared to the control sample (8.8 mm). Several researchers [77,83,84] reported that the voids ratio was found to reduce with inclusion of the nanomaterials in the cement matrix, resulting denser C-(A)-S-H gels. The reduction in the voids content can affect positively, thus lowering the porosity of the proposed mortars and reducing the CD. For all the proposed AAMs containing WBGNP up to 10%, the increment in the CD was found to be directly proportional to the contents of nanomaterials. The observed increase in CD value of the mortars from 8.3 mm to 9.4 mm with the corresponding increase of WBGNP level from 10% to 20% clearly indicated the significant impact of WBGNP inclusion in the mortar. Basheer et al. [85] made similar observation and it was found that the rate of carbonation within concrete is primarily determined by the AAS to binder ratio, as well as the porosity and carbon dioxide transport within a mortar matrix. Common knowledge dictates that the carbonation propagation is a process of CO<sub>2</sub> diffusion, moving from the environment into the mortar and the CD increases when there is an increase in the diffusion depth of CO<sub>2</sub>. Other than the environmental factors, carbonation within the mortar/concrete is also an occurring phenomenon due to the pore networks and micro cracks that exist within the concrete specimens, thus providing the routes for CO<sub>2</sub> diffusion.

Fig. 11 depicts the relationship between WA and CD of the AAMs exposed to CO<sub>2</sub> environment for 90 days. The measured CD were found to be directly proportional to the porosity of proposed mortars [86]. Huseien and Shah [87] reported that the nature and density of pores in the binder can influence the CD and WA negatively wherein the presence of non-interlinked pores in the mortar matrix may allow in intake of excess CO<sub>2</sub>, thus lowering emission level. The linear regression method (with R<sup>2</sup> values 0.95) was applied to correlate the experimental data which signified good confidence following the expression:

$$CD = 0.9457 WA - 0.7327 \quad (5)$$

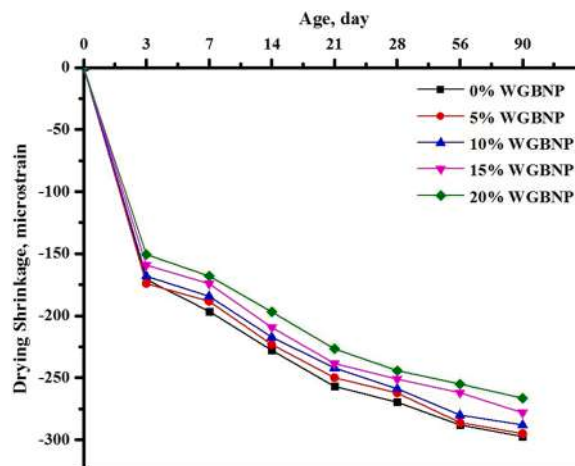


Fig. 9. Effect of WBGNP content on DS performance of AAMs.

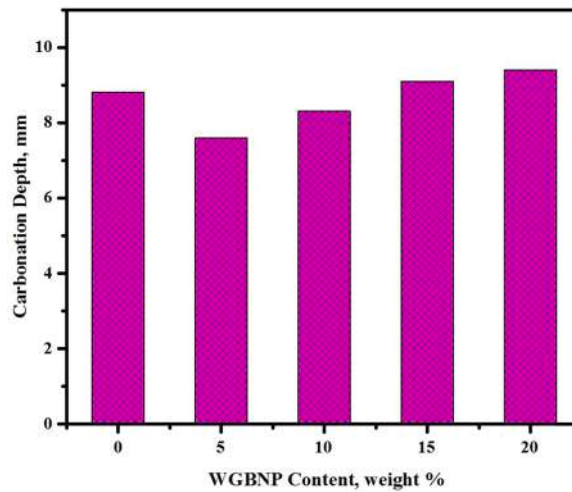


Fig. 10. CD of AAMs prepared with various levels of WGBNP as GBFS replacement.

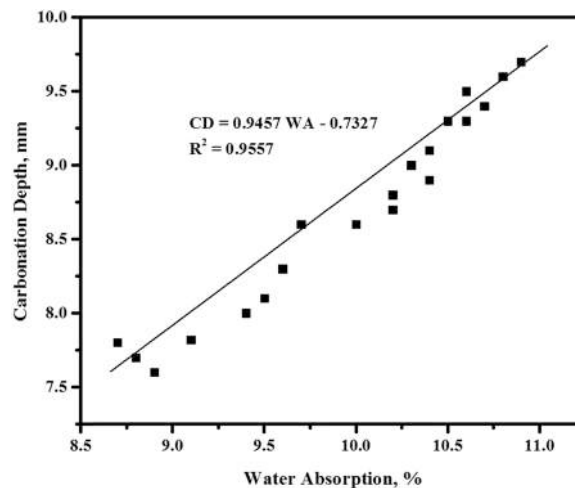


Fig. 11. Relationship between WA and CD of AAMs.

### 3.6. Abrasion resistance

Figs. 12 and 13 illustrates the effect of WGBNP incorporation at varying contents as GBFS replacement on the AR of AAMs. It is worth noting that at present the production of sustainable construction materials has been one of the main concerns to researchers in construction industry. One of the most important durability issues for the hydraulic structures is abrasion erosion (wear), which is considered to determine the service life of hydraulic structures. The AR of concrete is the most important property since all the surfaces will interface to the water pressure directly. Abrasion erosion damage is caused by the friction and the impact of water-borne silt, sand, gravel, rocks, ice, and other debris on the concrete surface of a hydraulic structure. The AR of all mortars was improved with the prolongation in the curing ages. The highest abrasion resistance was achieved for the mortar made with 5% of WGBNP as GBFS replacement. After 7 days, the AR of mortars prepared with 5% and 10% of WGBNP were increased by 25.5% and 9.3% compared to the control sample, respectively. However, specimens containing 15% and 20% of WGBNP showed loss in AR by 8.7% and 18.6% for, respectively. After 28 days of age, the AR of the mortar prepared with 5% and 10% of WGBNP was increased and decreased by 7% and 2.6%, respectively. For the specimens prepared with WGBNP up to 10%, the results indicted an inverse relationship between AR and WGBNP content. The AR was decreased with the rise of the grind depth when WGBNP contents in the mortars were increased. The grind depth values were increased from 1.11 mm to 1.43 mm with the increase of WGBNP level from 10% to 20%, respectively. Comparable trends were observed for the mortars cured for 56 and 90 days wherein the highest AR was achieved for the mortar made with 5% of WGBNP.

Liu et al. [88] found that the mortar with the wear porosity, high CS and strong interfacial bonds in the hardened paste can improve the mortar AR performance. With the reduction of mortars porosity, they appear more resistant, thus increasing the AR value. It was

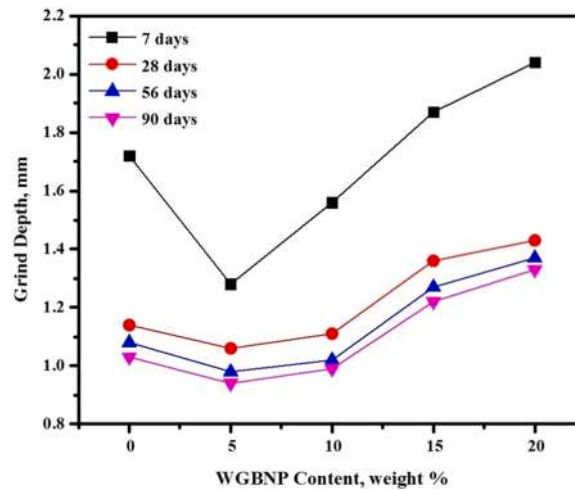


Fig. 12. WGBNP contents dependent AR of AAMs.

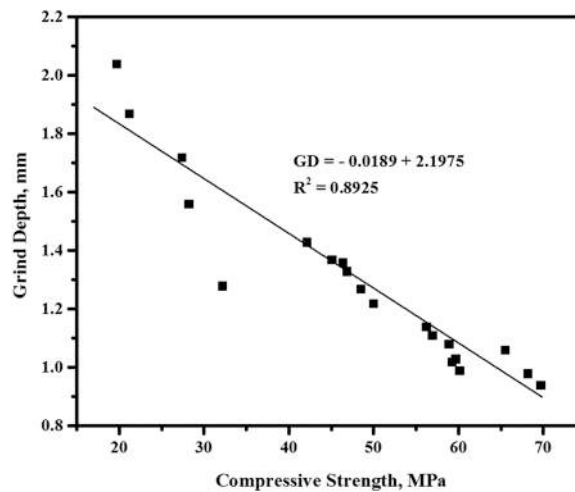


Fig. 13. AR and CS correlation of AAMs.

also reported that [89] CS can be reduced with the increase of pores volume in the hardened specimens, thus affecting negatively the value of AR. The grind depth (GD, a measure in the loss of AR) of the studied mortars was shown to be inversely proportional to CS. The experimentally measured AR or GD and CS data were correlated using the following linear regression relation with excellent confidence ( $R^2$  value of 0.89):

$$GD = -0.0189 \text{ CS} + 2.1975 \quad (6)$$

### 3.7. Resistance to freeze-thaw cycles

Resistance of mortar/concrete to freezing-thawing cycles is very important to measure their durability performance under aggressive environments. In this study, the resistance of the 28 days cured specimens was evaluated with 300 freeze/thaw cycles. The CS loss, weight loss, change in ultrasonic pulse velocity (UPV) and surface deteriorations were evaluated after every 50 freezing-thawing cycles. The influence of WGBNP as GBFS replacement on the freezing-thawing resistance of AAMs was widely assessed to determine the mortars' durability. Besides, the WGBNP content dependent CS loss, interior frost damages, and surface-scaling of the mortars were examined. Figs. 14, 15 and 16 show the influence of WGBNP inclusion by 0%, 5%, 10%, 15% and 20% in place of GBFS on the durability characteristics of AAMs.

Fig. 14 illustrates the loss in CS of evaluated specimens. It was found that the loss in CS trend to increase with increasing number of freezing-thawing cycles for all mortar mixtures. After 300 cycles, it was found that the replacement of GBFS by 5% of WGBNP led to

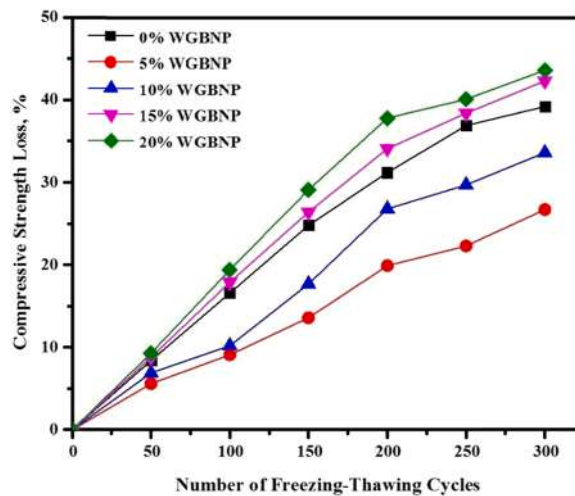


Fig. 14. CSL of AAMs under 300 freezing-thawing cycles after 28 days.

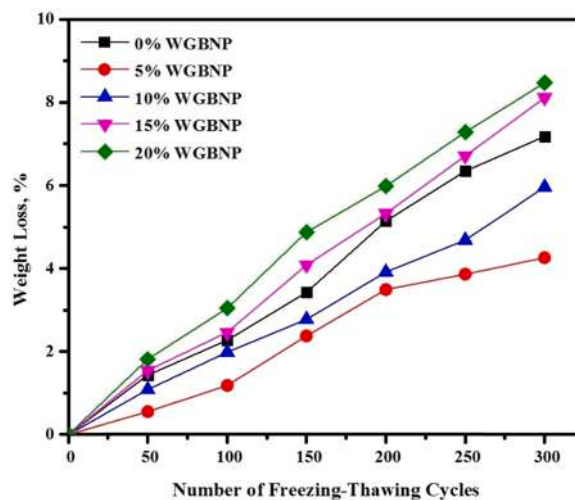


Fig. 15. Weight loss of AAMs under 300 freezing-thawing cycles after 28 days.

improve the durability performance and reduced the loss in strength from 39.2% to 26.7%. However, increase in the WGBNP content from 10% to 20% caused an increase in the loss in CS from 33.6% to and 43.6%, respectively. Clearly, 5% of WGBNP addition was the optimum amount to enhance the mortars' resistance to freezing-thawing cycles.

Fig. 15 shows the weight loss of AAM designed with different levels of WGBNP and exposed to 300 freezing-thawing cycles at 28 days of curing age. For all mortar specimens, it was observed that the weight loss increased with increasing number of freezing-thawing cycles. The weight loss was dropped from 7.2% to 5.9% with the increase of GBFS replacement level by WGBNP from 0% to 10%, respectively. Conversely, with the increase of WGBNP contents to 15% and 20%, the durability performance of AAMs was reduced and recorded weight loss was 8.1% and 8.5%, respectively. In comparison to the control sample, the mortar designed with 5% of WGBNP displayed the lowest weight loss and showed high durability, indicating its suitability to design high performance mortars required for the aggressive environments. The obtained enhancement of the mortars' resistance to freezing-thawing cycles with the inclusion of 5% WGBNP as GBFS replacement was mainly due to the improvement of the hydration process. It was inferred that the optimum content of nanomaterial can formulate dense surface with lower porosity, achieving highest performance. As mentioned in Section 3.2, the porosity of AAMs was reduced and the pores were refined with the increase of WGBNP level from 0% to 5%, reducing the ice formation [90]. Meanwhile, the pores became more detached, lowering the capillary-mediated transports of outside fluid in the concrete's pores during the freeze-thaw cycles. Consequently, less ice was nucleated which was mainly responsible for the surface-scaling regulated by the cryogenic suction of the interfacial fluid subjected to freeze cycles [91].

The UPV test was conducted to evaluate the internal cracks and deterioration of AAMs exposed to 50, 100, 150, 200, 250 and 300 of freezing-thawing cycles and the results are depicted in Fig. 16. For all the AAMs, deterioration was more pronounced with the increase in the number of freezing-thawing cycles. The UPV readings tend to decrease with the increase of exposure time, indicating the

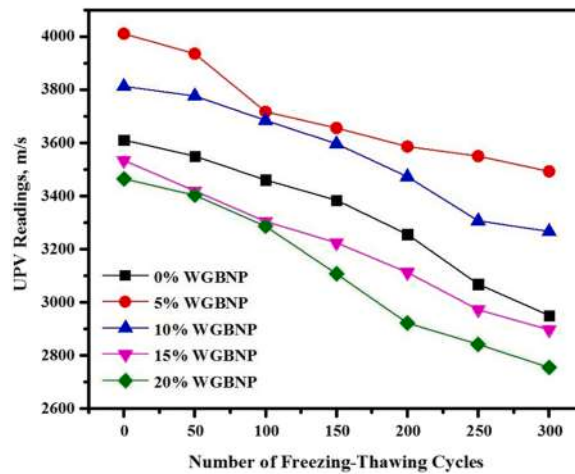


Fig. 16. Impact of WGBNP inclusion on UPV of AAMs.

creation of more internal cracks due to the ice expansion. The specimens designed using 5% and 10% of WGBNP displayed superior performances compared to the one devoid of WGBNP (control specimen). However, when the WGBNP content was increased to 10%, the deterioration of the mortar became more pronounced, thus reducing the resistance to freezing-thawing cycles. With the increase in the number of cycles, the damages on the surface and edge of the mortars were apparent (Fig. 17). Higher amount of deterioration was observed for specimen containing 20% of WGBNP as GBFS replacement. It is well known that an increase in the silica content and

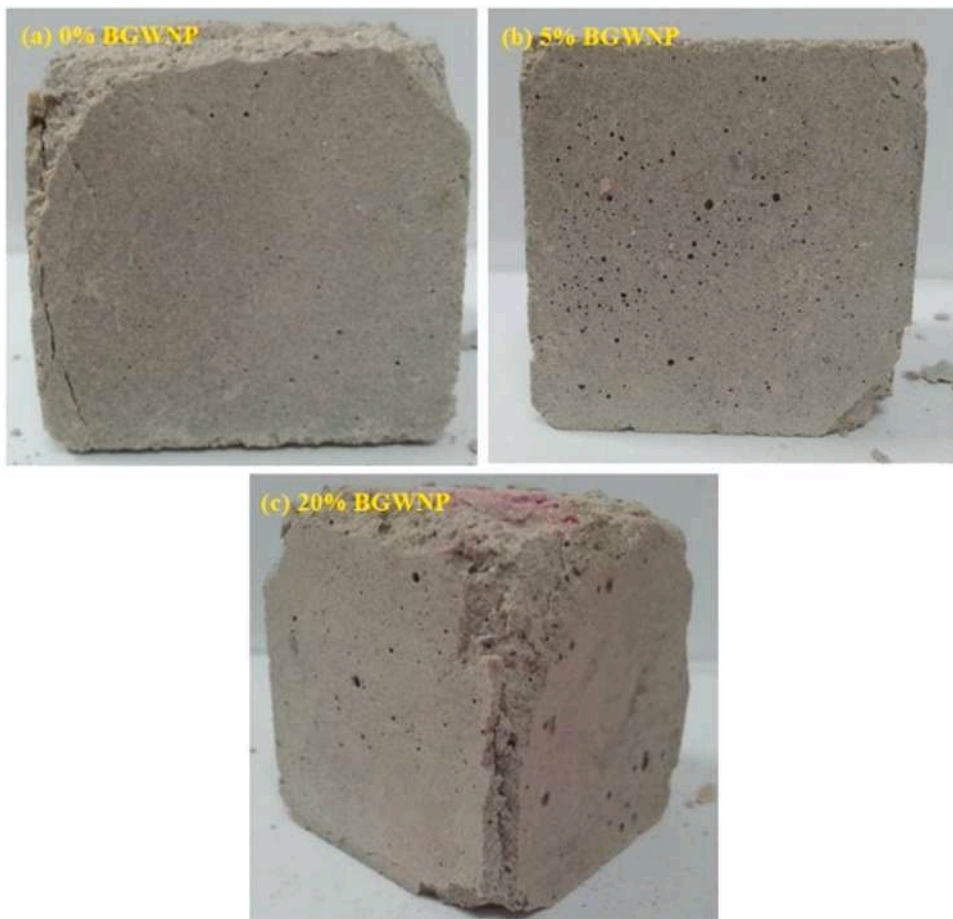


Fig. 17. Effect of freeze-thaw cycles on the surface texture of AAMs containing WGBNP as GBFS replacement.

reduction in calcium content can increase the porosity, thus leading to more deterioration. Furthermore, the increase in the voids in AAMs structure during the freezing-thawing cycles enabled to destroy the interlock between mortar particles, causing a loss in the bond strength [92,93].

Fig. 18 illustrates the relationship between resistance to freezing-thawing cycles in term of compressive strength loss (CSL) and porosity of AAMs. An increase in the porosity has led to reduce the specimen's resistance to freezing-thawing cycles. A linear relation was established between resistance to freezing-thawing cycles and porosity of mortars with a good  $R^2$  values around 0.96 as follows:

$$\text{CSL} = 8.8828 \text{ WA} - 51.501 \quad (7)$$

### 3.8. Resistance against acid attack

The chemical composition of alkali-activated binder strongly affected the performance of AAMs when exposed to sulphuric acid ( $\text{H}_2\text{SO}_4$ ) environment. The AAMs resistance against acid attacks was determined through the visual appearance, change of microstructures, loss of CS (Fig. 19), loss of weight (Fig. 20), loss of UPV readings (Fig. 21). For this purpose, the AAM specimens were exposed to 10% of  $\text{H}_2\text{SO}_4$  solution for 180 and 365 days to evaluate the effect of WGBNP content on the acid attack resistance of the prepared mortars. For all AAMs, the deterioration levels were discerned to reduce with the increase of WGBNP contents. At 28 days of curing, the AAMs were immersed in the acid solution with concentration of 10% and were evaluated after 180 and 365 days. Fig. 19 shows the impact of WGBNP contents on the compressive strength loss (CSL) of AAMs. After the immersion for 180 days, the CSL of the mortars was decreased from 5.2% to 2.4% with the corresponding increase of WGBNP contents from 0% to 20%. Likewise, the durability performance of AAMs tested after 365 days exhibited an enhancement with the increase of WGBNP level. The CSL was dropped from 15.1% to 7.3% with the corresponding increase of WGBNP contents from 0% to 20%. The inclusion of WGBNP as GBFS replacement in the AAMs contributed to enhance the resistance to acid solution and controlled the deterioration of the mortars (Fig. 20). The weight loss percentage was decreased slightly from 0.36% to 0.16% with the corresponding increase of WGBNP content from 0% to 20%. After 365 days, the increase of WGBNP from 5% to 20% in the alkali-activated matrix enhanced its resistance and reduced its weight loss from 0.4% to 0.23% compared to 0.49% for the control sample. It could be concluded that the WGBNP reduces the internal cracks (as shown from UPV reading results in Fig. 21) and improves the durability properties of mortars.

In general, the increasing WGBNP contents in the alkali-activated matrix as GBFS replacement had appreciable effect in reducing the calcium content. Several researchers [94–96] reported that the deterioration can cause the strength loss, expansion, spalling of surface layers and eventual disintegration. Most experts attributed the sulphate attack to the formation of expansive ettringite ( $3\text{CaO}\cdot\text{Al}_2\text{O}_3\cdot3\text{CaSO}_4\cdot32\text{H}_2\text{O}$ ) and gypsum [calcium sulphate dehydrate ( $\text{CaSO}_4\cdot2\text{H}_2\text{O}$ )], which may be due to the expansion or softening of the mortars' matrix. Various studies were conducted to evaluate the effect of calcium level on the durability performance of AAS under acidic environments [7,30]. Huseien et al. [30] assessed the influence of GBFS content (as calcium resource) on the acid resistance of ternary blended AAS incorporated with waste ceramic powder (WCP) and FA. The reduction in the GBFS level was shown to improve the durability and reduce the CSL of the studied specimens.

Fig. 22 shows the deterioration in the tested AAM cubes after 365 days of exposure to 10% of sulphuric acid solution. The surface deterioration, cracks' numbers and sizes were decreased with the increase of WGBNP content as GBFS replacement. It is well known that nanosilica can reduce the amount of calcium oxide, thus enhancing the mortars' resistance against acid attack through the reduction of porosity due to the restriction in calcium hydroxide formulation. Upon exposing the AAMs to sulphuric acid, the  $\text{Ca}(\text{OH})_2$  compound in mortar was reacted with  $\text{SO}_4^{2-}$  ions and formed gypsum ( $\text{CaSO}_4\cdot2\text{H}_2\text{O}$ ). This caused the expansion of the alkali-activated

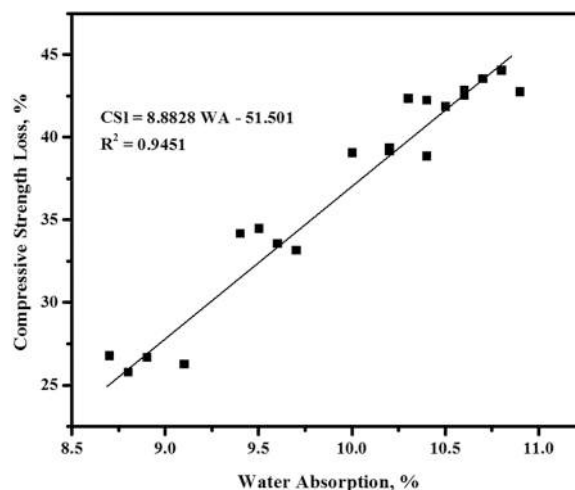


Fig. 18. CSL and porosity correlation of AAMs exposed to 300 freezing-thawing cycles.

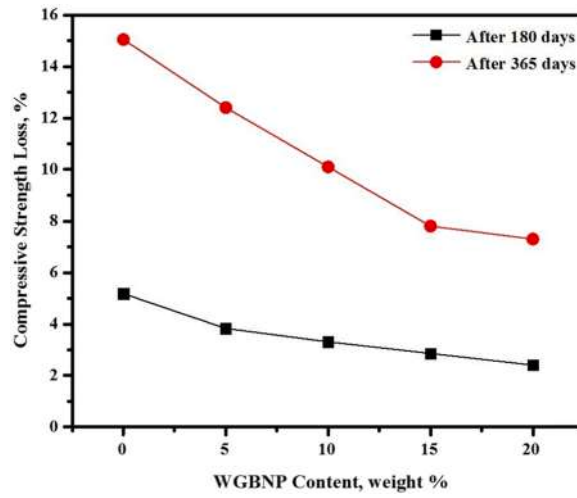


Fig. 19. Effect of 10% of H<sub>2</sub>SO<sub>4</sub> solution exposure on CSL of AAMs.

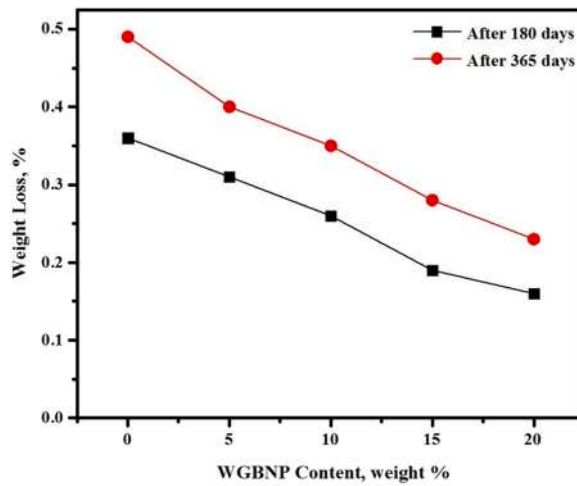


Fig. 20. Effect of 10% of H<sub>2</sub>SO<sub>4</sub> solution exposure on weight loss of AAMs.

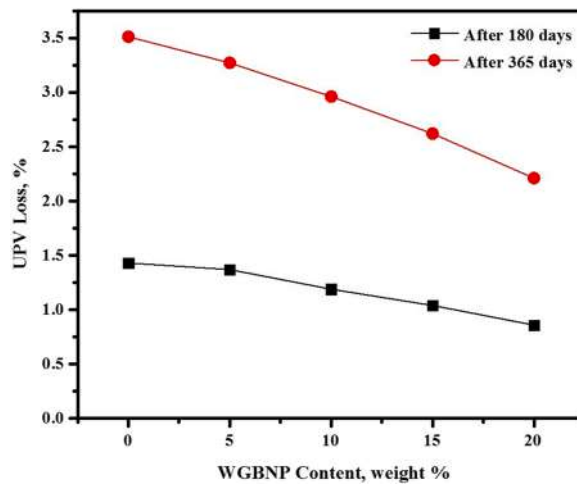


Fig. 21. Effect of 10% of H<sub>2</sub>SO<sub>4</sub> solution exposure on UPV reading loss of AAMs.

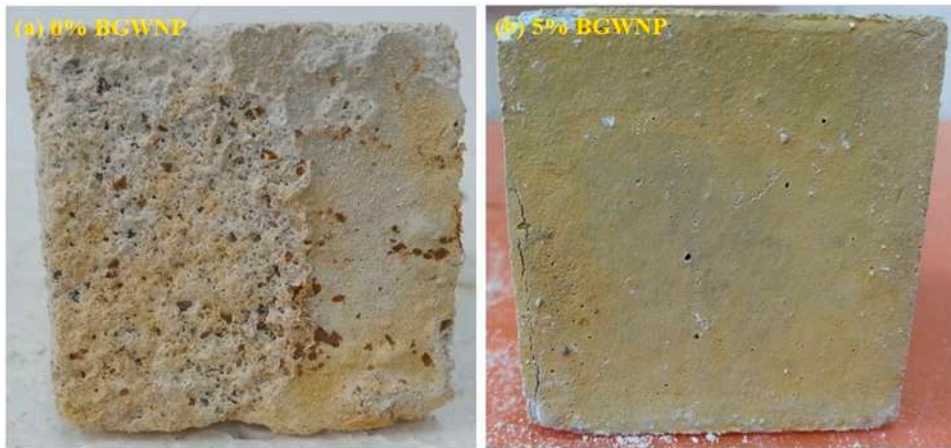


Fig. 22. Effect of 10% of  $H_2SO_4$  solution exposure on the surface textures of AAMs.

matrix and additional cracking in the interior of the specimens as reflected in the visual appearance (Fig. 22). It was indicated that [97–100] the reduction in CaO levels can lower the formation of Portlandite and gypsum, therefore improving the resistance of AAMs against sulphuric acid attacks.

The effect of 5% of WGBNP (optimum amount) as GBFS replacement on the XRD patterns of the proposed mortars exposed to 10% of  $H_2SO_4$  solution for 365 days were examined (Fig. 23). The mortar enclosing 0% of WGBNP still showed the major crystalline phases together with gypsum, quartz and reinhardbraunsite. The most intense XRD peaks (at  $26.8^\circ$ ,  $40^\circ$  and  $50^\circ$ ) corresponded to the crystalline phase of  $SiO_2$ . The observed new peaks at  $12.8^\circ$ ,  $16^\circ$ ,  $20.7^\circ$  and  $22.4^\circ$  in the mortar prepared with 0% of WGBNP were due gypsum, and gismondine crystallites. Another new peak appeared at  $30.9^\circ$  and  $31.4^\circ$  corresponded to the crystalline phase of reinhardbraunsite. However, the mortar prepared with 5% of WGBNP did not show any significant variation of the XRD profiles before and after the  $H_2SO_4$  solution exposure. The XRD analysis clearly indicated that the WGBNP inclusion as GBFS replacement in the mortar significantly enhanced their resistance against  $H_2SO_4$  attack. It is worth to ascertain a relationship between the deterioration rate of AAMs under  $H_2SO_4$  exposure and WGBNP levels as substitution agent for GBFS.

#### 4. Conclusions

The durability performance of a new type of sustainable AAMs was evaluated in terms of WA, CD, AR and DS, resistance to freeze-thaw cycles and acid attacks. These AAMs were designed by blending WGBNP, FA and GBFS, wherein various contents of WGBNP was incorporated as GBFS replacement. Depending on the experimental observations the conclusions are as follows:

- i. Inclusion of WGBNP of 10% as GBFS replacement in the mortar was shown to reduce the porosity and WA, thus enhancing the mortars' durability. Increase in the WGBNP contents to 5% and 20% could enhance the reaction process and produce denser C-(A)-S-H gels, further improving the microstructures with reduced pores.
- ii. An inverse correlation was established among the CS and porosity for the studied AAMs. Inclusion of 5% WGBNP as GBFS replacement in the mortars' matrix was found to enhance their microstructures and CS, reducing the porosity by 14.7% compared to the control sample.
- iii. Addition of 5% of WGBNP in the proposed AAMs enhanced the durability performance against the reduction of CD, establishing a linear relationship between the porosity and CD.
- iv. The replacement of GBFS by WGBNP was responsible for the lowering of the DS and durability performance improvement.
- v. Proposed mortar containing 5% of WGBNP displayed the highest performance related to freezing-thawing cycles, wherein the porosity reduction in AAMs enabled to increase the resistance to freezing-thawing cycles.
- vi. Direct relationship was ascertained between mortars' AR (wearing) and CS. Mortar containing 5% of WGBNP as GBFS replacement disclosed the highest wearing.
- vii. Proposed mortars containing WGBNP showed quite high resistance to sulphuric acid attack which was increased with the increase of WGBNP level. The minimum strength loss of 7.3% was achieved for AAMs containing 20% of WGBNP as GBFS replacement.
- viii. The detailed microstructures analyses (using XRD) of the WGBNP incorporated mortars displayed the formation of fewer amounts of free Portlandite and gypsum, reduction in the porosity and improvement in the durability performance against sulphuric acid attack.

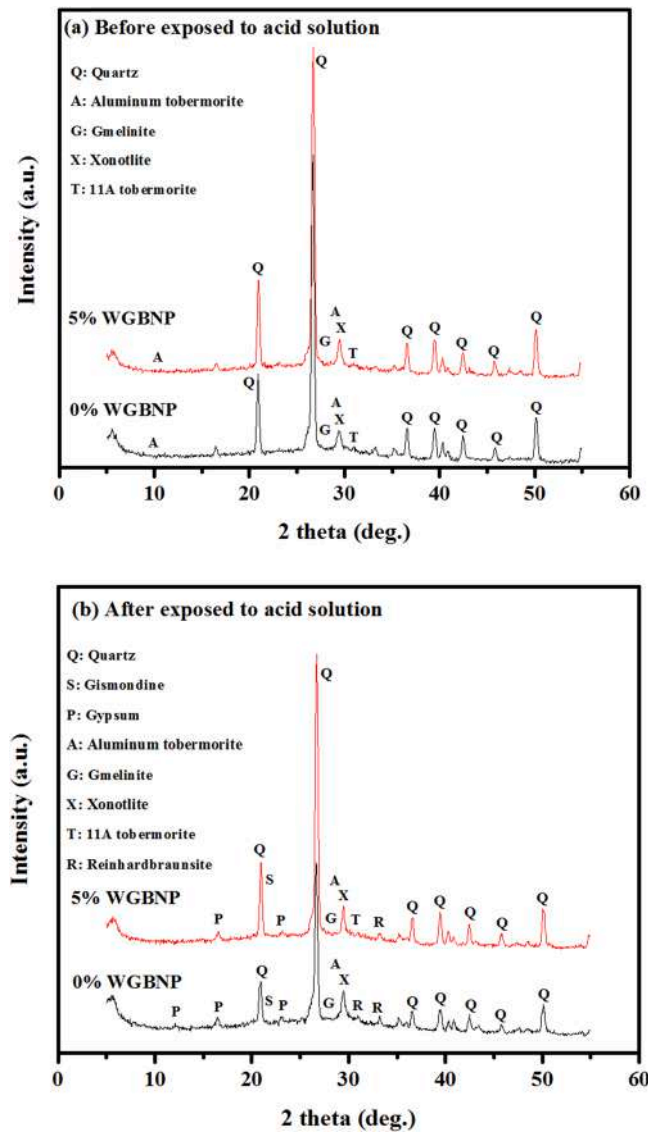


Fig. 23. XRD patterns of mortars (a) before (b) after 365 days of  $H_2SO_4$  solution exposure.

### Declaration of Competing Interest

The authors declare that they have no known competing financial interests or personal relationships that could have appeared to influence the work reported in this paper.

### Acknowledgements

Financial supports through the Universiti Teknologi Malaysia Fundamental Research (UTMFR) grant vot. 20H65 is gratefully appreciated. Also, the authors gratefully acknowledges the support of Researchers Supporting Project number (RSP-2021/290), King Saud University, Riyadh, Saudi Arabia

### References

- [1] M. Samadi, G.F. Huseien, H. Mohammadhosseini, H.S. Lee, N.H. Abdul Shukor Lim, M.M. Tahir, R. Alyousef, Waste ceramic as low cost and eco-friendly materials in the production of sustainable mortars, *J. Clean. Prod.* 266 (2020), 121825.
- [2] A. de Azevedo, A. Cruz, M.T. Marvila, L.B. de Oliveira, S.N. Monteiro, C. Vieira, R. Fediuk, R. Timokhin, N. Vatin, M. Daironas, Natural fibers as an alternative to synthetic fibers in reinforcement of geopolymer matrices: a comparative review, *Polymers* 13 (15) (2021) 2493.
- [3] G.F. Huseien, K.W. Shah, Performance evaluation of alkali-activated mortars containing industrial wastes as surface repair materials, *J. Build. Eng.* 30 (2020), 101234.

- [4] H. Mohammadhosseini, M.M. Tahir, M. Sayyed, Strength and transport properties of concrete composites incorporating waste carpet fibres and palm oil fuel ash, *J. Build. Eng.* 20 (2018) 156–165.
- [5] A. Azevedo et al., Characterization of waste from ornamental stones for use in mortar, in: *Characterization of Minerals, Metals and Materials*, 2014, pp. 379–386.
- [6] G. Azevedo, et al., Analysis of rheological behavior by the method squeeze flow in mortars incorporated with ornamental stone residue. *Characterization of Minerals, Metals, and Materials*, Springer, 2019, pp. 465–472.
- [7] K.W. Shah, G.F. Huseien, Bond strength performance of ceramic, fly ash and GBFS ternary wastes combined alkali-activated mortars exposed to aggressive environments, *Constr. Build. Mater.* 251 (2020), 119088.
- [8] A.R. de Azevedo et al., Effect of the addition and processing of glass polishing waste on the durability of geopolymeric mortars, *Case Stud. Constr. Mater.* 15 (2021) e00662.
- [9] A.R.G. de Azevedo, J. Alexandre, E.B. Zanelato, M.T. Marvila, Influence of incorporation of glass waste on the rheological properties of adhesive mortar, *Constr. Build. Mater.* 148 (2017) 359–368.
- [10] A.R.G. Azevedo, M.T. Marvila, H.A. Rocha, L.R. Cruz, C.M.F. Vieira, Use of glass polishing waste in the development of ecological ceramic roof tiles by the geopolymerization process, *Int. J. Appl. Ceram. Technol.* 17 (6) (2020) 2649–2658.
- [11] A.R.G. de Azevedo, M. Teixeira Marvila, L. Barbosa de Oliveira, W. Macario Ferreira, H. Colorado, S. Rainho Teixeira, C. Mauricio Fontes Vieira, Circular economy and durability in geopolymers ceramics pieces obtained from glass polishing waste, *Int. J. Appl. Ceram. Technol.* 18 (2021) 1891–1900.
- [12] M.T. Marvila, A. Azevedo, P.R. Matos, S.N. Monteiro, C. Vieira, Rheological and the fresh state properties of alkali-activated mortars by blast furnace slag, *Materials* 14 (8) (2021) 2069.
- [13] I. Faridmehar, C. Bedon, G. Huseien, M. Nikoo, M. Baghban, Assessment of mechanical properties and structural morphology of alkali-activated mortars with industrial waste materials, *Sustainability* 13 (4) (2021) 2062.
- [14] G.F. Huseien, A.R.M. Sam, K.W. Shah, M.A. Asaad, M.M. Tahir, J. Mirza, Properties of ceramic tile waste based alkali-activated mortars incorporating GBFS and fly ash, *Constr. Build. Mater.* 214 (2019) 355–368.
- [15] M. Izquierdo, X. Querol, J. Davidovits, D. Antenucci, H. Nugteren, C. Fernández-Pereira, Coal fly ash-slag-based geopolymers: microstructure and metal leaching, *J. Hazard. Mater.* 166 (1) (2009) 561–566.
- [16] M.T. Marvila et al., Mechanical, physical and durability properties of activated alkali cement based on blast furnace slag as a function of % Na<sub>2</sub>O, *Case Stud. Constr. Mater.* (2021) e00723.
- [17] P. Nath, P.K. Sarker, Effect of GGBFS on setting, workability and early strength properties of fly ash geopolymer concrete cured in ambient condition, *Constr. Build. Mater.* 66 (2014) 163–171.
- [18] A. Islam, U.J. Alengaram, M.Z. Jumaat, I.I. Bashar, The development of compressive strength of ground granulated blast furnace slag-palm oil fuel ash-fly ash based geopolymer mortar, *Mater. Des.* 56 (2014) 833–841.
- [19] G.F. Huseien, A.R.M. Sam, R. Alyousef, Texture, morphology and strength properties of self-compacting alkali-activated concrete: role of fly ash as GBFS replacement, *Constr. Build. Mater.* 270 (2021), 121368.
- [20] R. Sahana, Setting time compressive strength and microstructure of geopolymer paste, in: *Proceedings of the International Conference on Energy and Environment (ICEE'13)*, 2013.
- [21] P.S. Deb, P. Nath, P.K. Sarker, The effects of ground granulated blast-furnace slag blending with fly ash and activator content on the workability and strength properties of geopolymer concrete cured at ambient temperature, *Mater. Des.* 62 (2014) 32–39.
- [22] N. Marjanović, M. Komljenović, Z. Baščarević, V. Nikolić, R. Petrović, Physical–mechanical and microstructural properties of alkali-activated fly ash–blast furnace slag blends, *Ceram. Int.* 41 (1) (2015) 1421–1435.
- [23] M.H. Al-Majidi, A. Lampropoulos, A. Cundy, S. Meikle, Development of geopolymer mortar under ambient temperature for in situ applications, *Constr. Build. Mater.* 120 (2016) 198–211.
- [24] P. Nath, P.K. Sarker, V.B. Rangan, Early age properties of low-calcium fly ash geopolymer concrete suitable for ambient curing, *Procedia Eng.* 125 (2015) 601–607.
- [25] Z. Li, S. Liu, Influence of slag as additive on compressive strength of fly ash-based geopolymer, *J. Mater. Civ. Eng.* 19 (6) (2007) 470–474.
- [26] M. Guerrieri, J.G. Sanjayan, Behavior of combined fly ash/slag-based geopolymers when exposed to high temperatures, *Fire Mater.* 34 (4) (2010) 163–175.
- [27] I. Ismail, S.A. Bernal, J.L. Provis, S. Hamdan, J.S.J. van Deventer, Microstructural changes in alkali activated fly ash/slag geopolymers with sulfate exposure, *Mater. Struct.* 46 (3) (2013) 361–373.
- [28] M. Chi, R. Huang, Binding mechanism and properties of alkali-activated fly ash/slag mortars, *Constr. Build. Mater.* 40 (2013) 291–298.
- [29] G.F. Huseien, A.R.M. Sam, J. Mirza, M.M. Tahir, M.A. Asaad, M. Ismail, K.W. Shah, Waste ceramic powder incorporated alkali activated mortars exposed to elevated temperatures: performance evaluation, *Constr. Build. Mater.* 187 (2018) 307–317.
- [30] G.F. Huseien, A.R.M. Sam, K.W. Shah, J. Mirza, M.M. Tahir, Evaluation of alkali-activated mortars containing high volume waste ceramic powder and fly ash replacing GBFS, *Constr. Build. Mater.* 210 (2019) 78–92.
- [31] N.A. Qambrani, M.M. Rahman, S. Won, S. Shim, C. Ra, Biochar properties and eco-friendly applications for climate change mitigation, waste management, and wastewater treatment: a review, *Renew. Sustain. Energy Rev.* 79 (2017) 255–273.
- [32] K.W. Shah, G.F. Huseien, Biomimetic self-healing cementitious construction materials for smart buildings, *Biomimetics* 5 (4) (2020) 47.
- [33] J.S.J. van Deventer, J.L. Provis, P. Duxson, D.G. Brice, Chemical research and climate change as drivers in the commercial adoption of alkali activated materials, *Waste Biomass Valoriz.* 1 (1) (2010) 145–155.
- [34] V.S. Nandi, F. Raupp-Pereira, O.R.K. Montedo, A.P.N. Oliveira, The use of ceramic sludge and recycled glass to obtain engobes for manufacturing ceramic tiles, *J. Clean. Prod.* 86 (2015) 461–470.
- [35] T.R. Naik, G. Moriconi, Environmental-friendly durable concrete made with recycled materials for sustainable concrete construction, in: *International Symposium on Sustainable Development of Cement, Concrete and Concrete Structures*, Toronto, Ontario, October 2005.
- [36] M. Hasanuzzaman, A. Rafferty, M. Sajjia, A.G. Olabi, M. Hasanuzzaman, A. Rafferty, M. Sajjia, A.G. Olabi, Properties of glass materials, in: *Reference Module in Materials Science and Materials Engineering*, 2016, pp. 1–12.
- [37] E. Axinte, Glasses as engineering materials: a review, *Mater. Des.* 32 (4) (2011) 1717–1732.
- [38] L. Li, F. Wang, Q. Liao, Y. Wang, H. Zhu, Y. Zhu, Synthesis of phosphate based glass-ceramic waste forms by a melt-quenching process: the formation process, *J. Nucl. Mater.* 528 (2020), 151854.
- [39] M. Mehdi Jalili, S. Yahya Mousavi, A.S. Pirayeshfar, Investigating the acoustic properties of carbon fiber-, glass fiber-, and hemp fiber-reinforced polyester composites, *Polym. Compos.* 35 (11) (2014) 2103–2111.
- [40] M. Rakshvir, S.V. Barai, Studies on recycled aggregates-based concrete, *Waste Manag. Res.* 24 (3) (2006) 225–233.
- [41] S.-B. Park, B.-C. Lee, Studies on expansion properties in mortar containing waste glass and fibers, *Cem. Concr. Res.* 34 (7) (2004) 1145–1152.
- [42] I.B. Topcu, M. Canbaz, Properties of concrete containing waste glass, *Cem. Concr. Res.* 34 (2) (2004) 267–274.
- [43] T.-C. Ling, C.-S. Poon, H.-W. Wong, Management and recycling of waste glass in concrete products: current situations in Hong Kong, *Resour. Conserv. Recycl.* 70 (2013) 25–31.
- [44] Y. Jani, W. Hogland, Waste glass in the production of cement and concrete—a review, *J. Environ. Chem. Eng.* 2 (3) (2014) 1767–1775.
- [45] Z. Kubba, E. Hewayde, G. Fahim Huseien, A. Rahman Mohd Sam, M. Ali Asaad, Effect of sodium silicate content on setting time and mechanical properties of multi blend geopolymer mortars, *J. Eng. Appl. Sci.* 14 (2019) 2262–2267.
- [46] N. Su, J. Chen, Engineering properties of asphalt concrete made with recycled glass, *Resour. Conserv. Recycl.* 35 (4) (2002) 259–274.
- [47] Z.Z. Ismail, E.A. Al-Hashmi, Reuse of waste iron as a partial replacement of sand in concrete, *Waste Manag.* 28 (11) (2008) 2048–2053.
- [48] C. Shi, K. Zheng, A review on the use of waste glasses in the production of cement and concrete, *Resour. Conserv. Recycl.* 52 (2) (2007) 234–247.

- [49] A. Mohajerani, J. Vajna, T.H.H. Cheung, H. Kurmus, A. Arulrajah, S. Horpibulsuk, Practical recycling applications of crushed waste glass in construction materials: a review, *Constr. Build. Mater.* 156 (2017) 443–467.
- [50] G.F. Huseien, M. Ismail, N.H.A. Khalid, M.W. Hussin, J. Mirza, Compressive strength and microstructure of assorted wastes incorporated geopolymer mortars: effect of solution molarity, *Alex. Eng. J.* 57 (4) (2018) 3375–3386.
- [51] H. Maraghechi, M. Maraghechi, F. Rajabipour, C.G. Pantano, Pozzolanic reactivity of recycled glass powder at elevated temperatures: reaction stoichiometry, reaction products and effect of alkali activation, *Cem. Concr. Compos.* 53 (2014) 105–114.
- [52] P. Indumathi, S. Shabhudeen, C. Saraswathy, Synthesis and characterization of nano silica from the Pods of *Delonix regia* ash, *Int. J. Adv. Eng. Technol.* 2 (4) (2011) 421–426.
- [53] Y. Qing, Z. Zenan, K. Deyu, C. Rongshen, Influence of nano-SiO<sub>2</sub> addition on properties of hardened cement paste as compared with silica fume, *Constr. Build. Mater.* 21 (3) (2007) 539–545.
- [54] P. Bai, P. Sharratt, T.Y. Yeo, J. Bu, A facile route to preparation of high purity nanoporous silica from acid-leached residue of serpentine, *J. Nanosci. Nanotechnol.* 14 (9) (2014) 6915–6922.
- [55] H. Lindgreen, M. Geiker, H. Krøyer, N. Springer, J. Skibsted, Microstructure engineering of Portland cement pastes and mortars through addition of ultrafine layer silicates, *Cem. Concr. Compos.* 30 (8) (2008) 686–699.
- [56] G. Quercia, G. Hüsen, H. Brouwers, Water demand of amorphous nano silica and its impact on the workability of cement paste, *Cem. Concr. Res.* 42 (2) (2012) 344–357.
- [57] L. Raki, J. Beaudoin, R. Alizadeh, J. Makar, T. Sato, Cement and concrete nanoscience and nanotechnology, *Materials* 3 (2) (2010) 918–942.
- [58] H.Z. Lopez-Calvo, P. Montes-Garcia, T.W. Bremner, M.D.A. Thomas, V.G. Jiménez-Quero, Compressive strength of HPC containing CNI and fly ash after long-term exposure to a marine environment, *Cem. Concr. Compos.* 34 (1) (2012) 110–118.
- [59] A. Grinyis, V. Bocullo, A. Gumuliauskas, Research of alkali silica reaction in concrete with active mineral additives, *J. Sustain. Archit. Civ. Eng.* 6 (1) 34–41.
- [60] Y. Ma, H. Fu, C. Zhang, S. Cheng, J. Gao, Z. Wang, W. Jin, J. Conde, D. Cui, Effect of nano-SiO<sub>2</sub> on the hydration and microstructure of Portland cement, *Nanomaterials* 6 (12) (2016) 241.
- [61] M.M. Norhasri, M. Hamidah, A.M. Fadzil, Applications of using nano material in concrete: a review, *Constr. Build. Mater.* 133 (2017) 91–97.
- [62] ASTM, C., 618 (1993) Standard specification for coal fly ash and raw or calcined natural pozzolan for use as a mineral admixture in concrete, in: *Annual Book of ASTM Standards*, Philadelphia, USA, 1999.
- [63] M.T. Marvila, A.R.Gd Azevedo, C.M.F. Vieira, Reaction mechanisms of alkali-activated materials, *Rev. IBRACON Estrut. Mater.* 14 (2021) 14.
- [64] M.T. Marvila, A. de Azevedo, P.R. de Matos, S.N. Monteiro, C. Vieira, Materials for production of high and ultra-high performance concrete: review and perspective of possible novel materials, *Materials* 14 (15) (2021) 4304.
- [65] M.A. Kewalramani, Z.I. Syed, Application of nanomaterials to enhance microstructure and mechanical properties of concrete, *Int. J. Integr. Eng.* 10 (2018) 2.
- [66] A.M. Onaizi, G.F. Huseien, N.H.A.S. Lim, M. Amran, M. Samadi, Effect of nanomaterials inclusion on sustainability of cement-based concretes: a comprehensive review, *Constr. Build. Mater.* 306 (2021), 124850.
- [67] M. Samadi, K.W. Shah, G.F. Huseien, N.H.A.S. Lim, Influence of glass silica waste nano powder on the mechanical and microstructure properties of alkali-activated mortars, *Nanomaterials* 10 (2) (2020) 324.
- [68] V.V. Vikulin, M.K. Alekseev, I.L. Shkarupa, Study of the effect of some commercially available nanopowders on the strength of concrete based on alumina cement, *Refract. Ind. Ceram.* 52 (4) (2011) 288–290.
- [69] A.M. Rashad, A synopsis about the effect of nano-Al<sub>2</sub>O<sub>3</sub>, nano-Fe<sub>2</sub>O<sub>3</sub>, nano-Fe<sub>3</sub>O<sub>4</sub> and nano-clay on some properties of cementitious materials—a short guide for Civil Engineer, *Mater. Des.* 52 (2013) 143–157.
- [70] A.M. Rashad, Effects of ZnO<sub>2</sub>, ZrO<sub>2</sub>, Cu<sub>2</sub>O<sub>3</sub>, CuO, CaCO<sub>3</sub>, SF, FA, cement and geothermal silica waste nanoparticles on properties of cementitious materials—a short guide for Civil Engineer, *Constr. Build. Mater.* 48 (2013) 1120–1133.
- [71] R. Zhang, X. Cheng, P. Hou, Z. Ye, Influences of nano-TiO<sub>2</sub> on the properties of cement-based materials: hydration and drying shrinkage, *Constr. Build. Mater.* 81 (2015) 35–41.
- [72] L. Wang, H. Zhang, Y. Gao, Effect of TiO<sub>2</sub> nanoparticles on physical and mechanical properties of cement at low temperatures, *Adv. Mater. Sci. Eng.* 2018 (2018) 1–12.
- [73] L. Wang, et al., Effect of nano-SiO<sub>2</sub>(2) on the hydration and microstructure of Portland cement, *Nanomaterials* 6 (12) (2016) 241.
- [74] M.M. Khotbehsara, E. Mohseni, M.A. Yazdi, P. Sarker, M.M. Ranjbar, Effect of nano-CuO and fly ash on the properties of self-compacting mortar, *Constr. Build. Mater.* 94 (2015) 758–766.
- [75] A. Nazari, S. Riahi, The effects of SiO<sub>2</sub> nanoparticles on physical and mechanical properties of high strength compacting concrete, *Compos. Part B Eng.* 42 (3) (2011) 570–578.
- [76] M. Morsy, S. Alsayed, M. Aqel, Hybrid effect of carbon nanotube and nano-clay on physico-mechanical properties of cement mortar, *Constr. Build. Mater.* 25 (1) (2011) 145–149.
- [77] N.H.A.S. Lim, H. Mohammadhosseini, M.M. Tahir, M. Samadi, A.R.M. Sam, Microstructure and strength properties of mortar containing waste ceramic nanoparticles, *Arab. J. Sci. Eng.* 43 (10) (2018) 5305–5313.
- [78] G.F. Huseien, H.K. Hamzah, A.R. Mohd Sam, N.H.A. Khalid, K.W. Shah, D.P. Deogrescu, J. Mirza, Alkali-activated mortars blended with glass bottle waste nano powder: environmental benefit and sustainability, *J. Clean. Prod.* 243 (2020) 243.
- [79] J.J. Thomas, H.M. Jennings, J.J. Chen, Influence of nucleation seeding on the hydration mechanisms of tricalcium silicate and cement, *J. Phys. Chem. C* 113 (11) (2009) 4327–4334.
- [80] S. Thokchom, P. Ghosh, S. Ghosh, Effect of water absorption, porosity and sorptivity on durability of geopolymer mortars, *ARPN J. Eng. Appl. Sci.* 4 (7) (2009) 28–32.
- [81] G.F. Huseien, A.R.M. Sam, K.W. Shah, A.M.A. Budiea, J. Mirza, Utilizing spend garnets as sand replacement in alkali-activated mortars containing fly ash and GBFS, *Constr. Build. Mater.* 225 (2019) 132–145.
- [82] A.K. Saha, Effect of class F fly ash on the durability properties of concrete, *Sustain. Environ. Res.* 28 (1) (2018) 25–31.
- [83] M. Samadi, G.F. Huseien, N.H.A.S. Lim, H. Mohammadhosseini, R. Alyousef, J. Mirza, A.B.A. Rahman, Enhanced performance of nano-palm oil ash-based green mortar against sulphate environment, *J. Build. Eng.* 32 (2020), 101640.
- [84] J. Tanzadeh, Laboratory evaluation of self-compacting fiber-reinforced concrete modified with hybrid of nanomaterials, *Constr. Build. Mater.* 232 (2020), 117211.
- [85] P. Basheer, 40 Designs of Concrete to Resist Carbonation, vol. 1, NRC Research Press, Ottawa, Canada, 1999.
- [86] Z. Farhana, et al., The relationship between water absorption and porosity for geopolymer paste, *Mater. Sci. Forum* (2015).
- [87] G.F. Huseien, K.W. Shah, Durability and life cycle evaluation of self-compacting concrete containing fly ash as GBFS replacement with alkali activation, *Constr. Build. Mater.* 235 (2020), 117458.
- [88] Y.-W. Liu, T. Yen, T.-H. Hsu, Abrasion erosion of concrete by water-borne sand, *Cem. Concr. Res.* 36 (10) (2006) 1814–1820.
- [89] S.-D. Wang, K.L. Scrivener, P. Pratt, Factors affecting the strength of alkali-activated slag, *Cem. Concr. Res.* 24 (6) (1994) 1033–1043.
- [90] J. Marchand, et al., Influence of chloride solution concentration on deicer salt scaling deterioration of concrete, *Mater. J.* 96 (4) (1999) 429–435.
- [91] Z. Liu, W. Hansen, Freezing characteristics of air-entrained concrete in the presence of deicing salt, *Cem. Concr. Res.* 74 (2015) 10–18.
- [92] H.Y. Shyu, C.J. Ko, Y.C. Luo, H.Y. Lin, S.R. Wu, S.W. Lan, T.S. Cheng, S.H. Hu, M.S. Lee, Experimental investigation on freeze-thaw durability of Portland cement pervious concrete (PCPC), *Constr. Build. Mater.* 117 (2016) 63–71.
- [93] N.P. Mayercsik, M. Vandamme, K.E. Kurtis, Assessing the efficiency of entrained air voids for freeze-thaw durability through modeling, *Cem. Concr. Res.* 88 (2016) 43–59.
- [94] M.O. Yusuf, Performance of slag blended alkaline activated palm oil fuel ash mortar in sulfate environments, *Constr. Build. Mater.* 98 (2015) 417–424.

- [95] M.A.R. Bhutta, W.M. Hussin, M. Azreen, M.M. Tahir, Sulphate resistance of geopolymer concrete prepared from blended waste fuel ash, *J. Mater. Civ. Eng.* 26 (11) (2014), 04014080.
- [96] S. Donatello, A. Fernández-Jimenez, A. Palomo, Very high volume fly ash cements. Early age hydration study using Na<sub>2</sub>SO<sub>4</sub> as an activator, *J. Am. Ceram. Soc.* 96 (3) (2013) 900–906.
- [97] M.A.B. Ahmed, et al., Performance of high strength POFA concrete in acidic environment, *Concr. Res. Lett.* 1 (1) (2010) 14–18.
- [98] M.A.M. Ariffin, M.A.R. Bhutta, M.W. Hussin, M. Mohd Tahir, N. Aziah, Sulfuric acid resistance of blended ash geopolymer concrete, *Constr. Build. Mater.* 43 (2013) 80–86.
- [99] S.O. Bamaga, M.A. Ismail, Z.A. Majid, M. Ismail, M.W. Hussin, Evaluation of sulfate resistance of mortar containing palm oil fuel ash from different sources, *Arab. J. Sci. Eng.* 38 (9) (2013) 2293–2301.
- [100] A. Noruzman, et al., Strength and durability characteristics of polymer modified concrete incorporating Vinyl acetate effluent, *Adv. Mater. Res.* (2013).